Generating orthogonally circular polarized states embedded in nonplanar geometric beams

T. H. Lu* and C. H. He

Department of physics, National Taiwan Normal University, 88 Tingchou Road, Sec. 4, Taipei 11677, Taiwan
**thlu@ntnu.edu.tw*

Abstract: We experimentally demonstrated the generation of orthogonally circular polarized states embedded in nonplanar geometric beams. Experimental results revealed that the production of circularly polarized beams, induced by crystal birefringence, is quantized. Numerical analyses of the polarization and the spatial morphology are consistent with the experimental results.

OCIS codes: (140.3480) Lasers, diode-pumped; (140.4780) Optical resonators; (260.5430) Polarization; (260.1440) Birefringence.

References and links

1. Q. Zhan, "Trapping metallic Rayleigh particles with radial polarization," Opt. Express **12**(15), 3377–3382 (2004).
2. A. Desyatnikov, T. A. Fadeyeva, V. G. Shvedov, Y. V. Izdebskaya, A. V. Volyar, E. Brasselet, D. N. Neshev, W. Krolikowski, and Y. S. Kivshar, "Spatially engineered polarization states and optical vortices in uniaxial crystals," Opt. Express **18**(10), 10848–10863 (2010).
3. H. Chen, Z. Zheng, B. F. Zhang, J. Ding, and H. T. Wang, "Polarization structuring of focused field through polarization-only modulation of incident beam," Opt. Lett. **35**(16), 2825–2827 (2010).
4. G. M. Lerman, L. Stern, and U. Levy, "Generation and tight focusing of hybridly polarized vector beams," Opt. Express **18**(26), 27650–27657 (2010).
5. A. B. Klimov, J. L. Romere, and S. Wallentowitz, "Quantum-state tomography for optical polarization with arbitrary photon numbers," Phys. Rev. A **89**(2), 020101 (2014).
6. L. Sansoni, F. Sciarrino, G. Vallone, P. Mataloni, A. Crespi, R. Ramponi, and R. Osellame, "Polarization Entangled State Measurement on a Chip," Phys. Rev. Lett. **105**(20), 200503 (2010).
7. D. Lin and W. A. Clarkson, "Polarization-dependent transverse mode selection in an Yb-doped fiber laser," Opt. Lett. **40**(4), 498–501 (2015).
8. Y. T. Yu, P. H. Tuan, K. F. Huang, and Y. F. Chen, "Exploring the influence of boundary shapes on emission angular distributions and polarization states of broad-area vertical-cavity surface-emitting lasers," Opt. Express **22**(22), 26939–26946 (2014).
9. Y. Kozawa, K. Yonezawa, and S. Sato, "Radially polarized laser beam from a Nd:YAG laser cavity with a *c*-cut YVO4 crystal," Appl. Phys. B **88**(1), 43–46 (2007).
10. T. H. Lu, Y. F. Chen, and K. F. Huang, "Generation of polarization-entangled optical coherent waves and manifestation of vector singularity patterns," Phys. Rev. E Stat. Nonlin. Soft Matter Phys. **75**(2), 026614 (2007).
11. K. Yonezawa, Y. Kozawa, and S. Sato, "Generation of a radially polarized laser beam by use of the birefringence of a *c*-cut Nd:YVO4 crystal," Opt. Lett. **31**(14), 2151–2153 (2006).
12. A. Ciattoni, G. Cincotti, and C. Palma, "Circularly polarized beams and vortex generation in uniaxial media," J. Opt. Soc. Am. A **20**(1), 163–171 (2003).
13. E. Brasselet, Y. Izdebskaya, V. Shvedov, A. S. Desyatnikov, W. Krolikowski, and Y. S. Kivshar, "Dynamics of optical spin-orbit coupling in uniaxial crystals," Opt. Lett. **34**(7), 1021–1023 (2009).
14. X. Lu and L. Chen, "Spin-orbit interactions of a Gaussian light propagating in biaxial crystals," Opt. Express **20**(11), 11753–11766 (2012).
15. T. H. Lu and L. H. Lin, "Observation of a superposition of orthogonally polarized geometric beams with a *c*-cut Nd:YVO4 crystal," Appl. Phys. B **106**(4), 863–866 (2012).
16. T. H. Lu, Y. C. Lin, H. C. Liang, Y. J. Huang, Y. F. Chen, and K. F. Huang, "Observation of lasing modes with exotic localized wave patterns from astigmatic large-Fresnel-number cavities," Opt. Lett. **35**(3), 345–347 (2010).
17. T. H. Lu, Y. C. Lin, Y. F. Chen, and K. F. Huang, "Three-Dimensional Coherent Optical Waves Localized on Trochoidal Parametric Surfaces," Phys. Rev. Lett. **101**(23), 233901 (2008).
18. Y. F. Chen, T. H. Lu, K. W. Su, and K. F. Huang, "Devil's staircase in three-dimensional coherent waves localized on Lissajous parametric surfaces," Phys. Rev. Lett. **96**(21), 213902 (2006).

#243787 Received 25 Jun 2015; revised 27 Jul 2015; accepted 29 Jul 2015; published 31 Jul 2015

1. Introduction

Polarization is a crucial laser beam characteristic influencing a wide range of laser beam applications, such as optical trapping [1], optical vortex generation [2], focus shaping [3,4], and quantum information transmission [5,6]. Generating space-variant polarization light has attracted considerable attention in the fields of fiber laser [7], vertical-cavity surface-emitting laser [8], and diode-pumped solid-state lasers [9,10]. The birefringence of a c-cut Nd:YVO_4 crystal has been used for generating radially and azimuthally polarized beams. Controlling the cavity length for the extraordinary and ordinary rays in a hemispherical cavity leads to different stability limits for these two rays [11]. This principle has been successfully exploited for the generation of low-order transverse vector beams. Furthermore, light beams in circularly polarized states carry spin angular momentum. Therefore, the generation of circularly polarized beams is of interest for studying optical vortex and optical spin-orbit coupling [12–14].

Apart from the eigenmodes of polarization states, superposed modes with orthogonally polarized states have been experimentally verified to localize on a two-dimensional geometric trajectory in a plano-concave cavity [15]. Base on the concept of degenerate cavities with an a-cut Nd:YVO_4 crystal, a hemispherical cavity is appropriate for superposed eigenmodes generation [16]. The stimulated emission cross-section and absorption coefficient of the a-cut Nd:YVO_4 crystal are 3.5 times and 4 times larger than those of the c-cut Nd:YVO_4 crystal, respectively, and therefore, the generation of superposed eigenmodes localized on classical trajectories of linear polarization is evident in the a-cut Nd:YVO_4 crystal [17]. Studies of the superposition of coherent waves have helped improve our understanding of quantum-classical correspondence. In view of the combined importance of polarization and superposed coherent waves, the generation of space-variant polarization states embedded in high-order superposed eigenmodes warrants research.

In this study, we demonstrated the generation of orthogonally circular polarized states from a diode-end-pumped c-cut Nd:YVO_4 laser. The longitudinal-transverse coupling effect leads to the localization of superposed eigenmodes on six coherent nonplanar beams in the propagation direction. The birefringence of the c-cut Nd:YVO_4 crystal requires the polarization continuity of the laser beams oscillating in the cavity. By adjusting the pump offset, the orthogonally circular polarized states embedded in the geometric beams can be experimentally quantized. To the best of our knowledge, this paper is the first to report the generation of orthogonally circular polarized states embedded in nonplanar geometric beams from a laser cavity.

2. Experimental setup and results

We used a diode-end-pumped laser system to accomplish the experiment. The experimental setup is depicted in Fig. 1. The laser resonator consisted of a plano-concave mirror with a radius of curvature (R) of 10 mm and a c-cut 2.0-at. % Nd:YVO_4 gain medium. The gain crystal was 1 mm in length, with a cross section of 3 mm x 3 mm. One side of the gain crystal was coated for antireflection at 1064 nm, and the other side was coated to be an output coupler with a reflectivity of 99%. The reflectivity of the front mirror was 99.8% at 1064 nm. The pump source was an 809 nm fiber-coupled laser diode with a core diameter of 105 μm , numerical aperture of 0.22, and maximum power of 3 W. A focusing lens with a focal length and coupling efficiency of 25mm and 80%, respectively, was used to reimage the pump beam into the laser crystal; it was mounted on a two-dimensional mechanical stage for adjusting the pump offset. The cavity length and pump offset were fixed at 7.6 mm and 590 μm , respectively. As increase in the pump offset led to the lasing beam gradually transforming from the fundamental Gaussian mode to a high-order mode localized on a nonplanar geometric trajectory formed by six coherent beams. Figures 1(a)–1(f) show the experimental results for the nonplanar geometric beams in the propagation direction. The middle of Fig. 1 illustrates the three-dimensional trajectory of the nonplanar geometric mode from the near

#243787 Received 25 Jun 2015; revised 27 Jul 2015; accepted 29 Jul 2015; published 31 Jul 2015

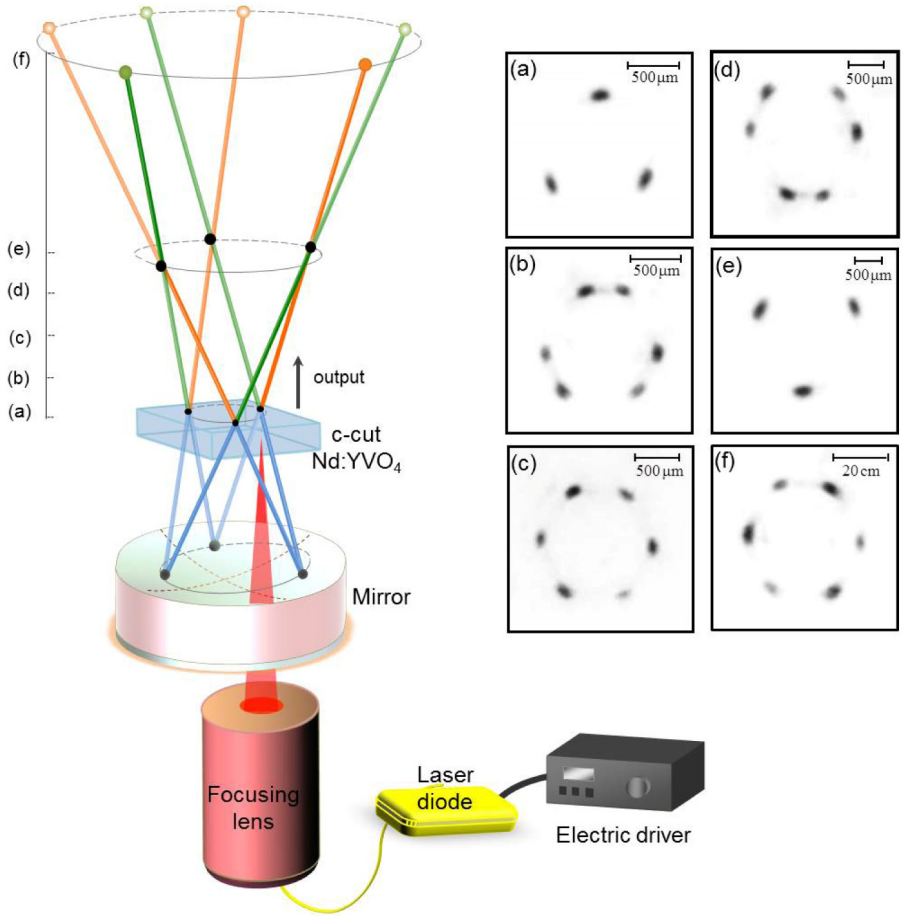

Fig. 1. Experimental setup and 3D trajectory of the circular geometric mode from the near field to the far field. Experimental transverse patterns of the 3D geometric mode at (a) $z = 0$, (b) $z = 1.15\,\text{mm}$, (c) $z = 2.48\,\text{mm}$, (d) $z = 4.27\,\text{mm}$, (e) $z = 7.39\,\text{mm}$, and (f) far field.

field to the far field. The nonplanar geometric beam in the cavity is symmetric Because the standing wave is the only wave in laser resonators, we consider nonplanar geometric modes propagating in opposite directions in the cavity. The orange and green lines in Fig. 1 represent the geometric mode propagating in the clockwise and counterclockwise directions, respectively. Experimental results revealed that the polarization states of the two circular geometric modes were right and left circularly polarized states, respectively. The coexistence of left and right circularly polarized states in a laser cavity is interesting. The experimental polarization-resolved far-field pattern shown in Fig. 2(b) indicates that the six spots of the nonplanar geometric modes correspond to the right and left circularly polarized states, respectively. The polarization dependence of the nonplanar geometric mode results from the interaction between the beam trajectory and the birefringent laser medium. The experimental results showed that coexisting oppositely circularly polarized states embedded in the nonplanar geometric beam are ubiquitous in the degenerate cavity with $L/R \approx 3/4$, where L is the cavity length. However, not every pump offset caused the formation of coexisting oppositely circularly polarized states. The formation of circularly polarized states was quantized in the laser cavity. An increase in the pump offset caused the lasing mode to discontinuously change from one nonplanar geometric mode to another nonplanar geometric

#243787 Received 25 Jun 2015; revised 27 Jul 2015; accepted 29 Jul 2015; published 31 Jul 2015

mode, implying that the circularly polarized states embedded in the geometric beam show polarization continuity in a round trip through the cavity containing a birefringent medium.

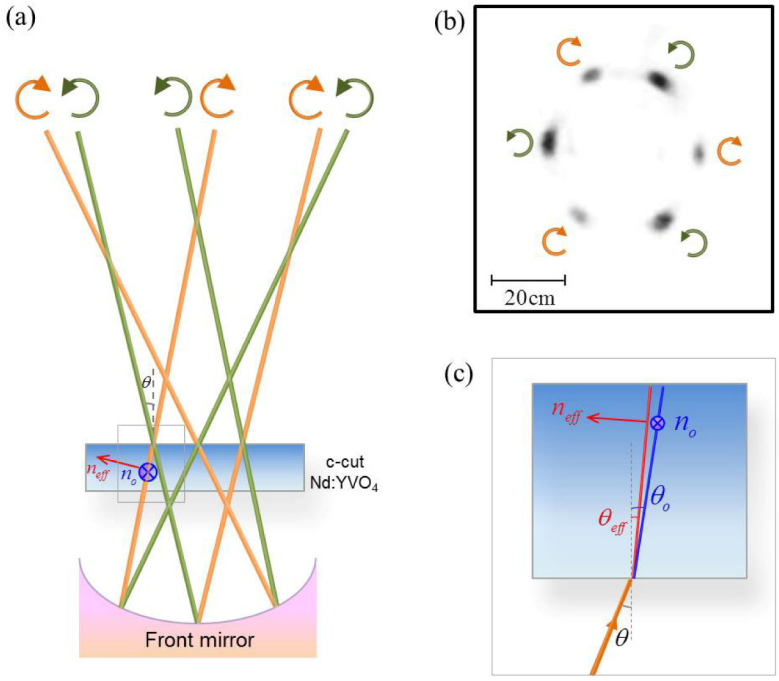

Fig. 2. (a) Side view of the nonplanar geometric mode with left and right circularly polarized states. (b) Experimental far field pattern. (c) Enlargement of the beam at an angle θ from the z axis, and the corresponding refractive indices.

3. Numerical analyses of polarization results

In a positive birefringent Nd:YVO_4 crystal with $n_o = 1.9573$ and $n_e = 2.1652$ at 1064 nm, strong polarization-dependent fluorescence emission exists because of the anisotropic crystal field. When a fundamental Gaussian-mode laser beam enters a c-cut Nd:YVO_4 crystal at an incident angle 0°, the birefringence is zero because of high-level transverse isotropy. Furthermore, when a laser beam enters the crystal at an angle θ with regard to the optic axis, the birefringence leads to a change in the polarization state according to the phase retardation. Figure 2(a) illustrates the side view of the nonplanar geometric mode in the propagation direction. The nonplanar geometric mode localized on six individual beams can be considered equivalent to multiple Gaussian beam oscillating in the cavity and passing through the crystal at the same angle θ. Depending on θ, the transverse electric fields related to the two refractive indices n_o and n_{eff} induce refractive angles θ_o and θ_{eff}. The effective refractive index n_{eff} is given by

$$n_{eff} = \frac{n_o n_e}{\sqrt{n_e^2 \cos^2\theta + n_o^2 \sin^2\theta}}. \quad (1)$$

The magnified diagram in Fig. 2(c) depicts the different paths of the two beams; however, the experimental lateral displacement of the two beams was sufficiently small to maintain the localized geometric mode. The difference between the two refractive indices leads to phase retardation, which is represented as

#243787 Received 25 Jun 2015; revised 27 Jul 2015; accepted 29 Jul 2015; published 31 Jul 2015

$$\delta = \left(\frac{2\pi \cdot d}{\lambda}\right)\left(\frac{n_{\text{eff}}}{\cos(\theta_{\text{eff}})} - \frac{n_{\text{o}}}{\cos(\theta_{\text{o}})}\right) \tag{2}$$

where d is the thickness of the laser medium and λ is the wavelength of the laser beam. For a resonant cavity, the phase change of the field induced by the birefrigent crystal should be an integral multiple of 2π; it is expressed as $\int k\, dz = 2\pi \cdot m$, where k is the wave number, m is an integer, and integral range is twice crystal length, implying that the phase retardation of the nonplanar geometric mode follows $2\delta = 2\pi \cdot m$. Each beam of the nonplanar geometric mode which passes through the crystal and reflects from the coating side remains the same handed circular polarization. To produce a nonplanar geometric mode in a degenerate cavity, tight focusing and controlling the off-axis pump scheme is crucial. When increasing the pump offset, the angle of the lasing beam makes the phase retardation to satisfy the quantized rule, and the nonplanar geometric mode with orthogonally circular polarized states are generated. The experimental results revealed that the polarization states of the nonplanar geometric mode satisfy the quantized condition. Figure 3 shows the discrete conditions for the generation of

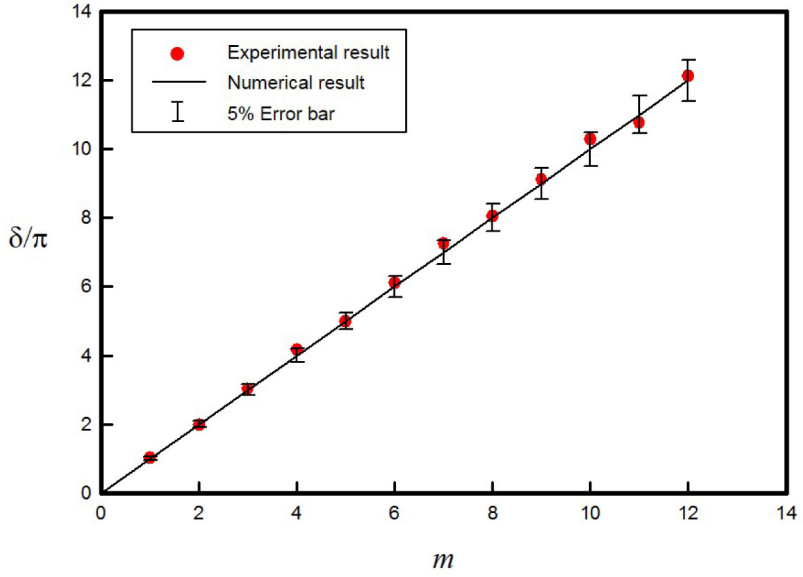

Fig. 3. Phase retardation values related to different m values. Dot: experimental result. Line: numerical result.

nonplanar geometric modes with orthogonally circular polarized states in the degenerate cavity of $L/R \approx 3/4$. The phase retardation values related to different m values represent the phase difference between the transverse orthogonal electric fields when the beam passes the gain medium at an incident angle relative to the optic axis. The error bar indicates a 5% range related to the numerical result. All error values lying within 5% demonstrate that the experimental data for phase retardation were in good agreement with the numerical analyses. The different m values represent the quantization of polarization continuity in the cavity; the polarization continuity facilitates the simultaneous formation of the orthogonally circular polarized states embedded in nonplanar geometric beams.

#243787 Received 25 Jun 2015; revised 27 Jul 2015; accepted 29 Jul 2015; published 31 Jul 2015

4. Numerical analyses of superposed Laguerre-Gaussian modes

A laser system with a pump offset and an *a*-cut Nd: YVO_4 crystal is typically characterized by the generation of Hermite-Gaussian (HG) modes and the mixing of HG modes [18]. By contrast, a laser system with a *c*-cut Nd: YVO_4 crystal typically generates Laguerre-Gaussian (LG) modes [11] and eigenmodes with elliptical coordinates [10]. The type of lasing mode depends on the symmetry of the boundary conditions (shape of the resonators and cavity length) and initial conditions (gain medium and pumping scheme). Since the YVO_4 crystal belongs to the group of oxide compounds crystallizing in a zircon structure with a tetragonal space group, the *c*-cut Nd:YVO_4 crystal is a high-level transverse isotropic crystal. Therefore, LG modes and the mixing of LG modes are appropriate bases for laser systems with a *c*-cut crystal. The wave function of an LG mode with longitudinal index s, transverse radial index p, and transverse azimuthal index l in cylindrical coordinates (ρ,ϕ,z) is given by $\Psi_{p,l,s}(\rho,\phi,z)=e^{il\phi}\Phi_{p,l,s}(\rho,z)$. Here,

$$\begin{aligned}\Phi_{p,l,s}(\rho,z)=&\sqrt{\frac{2p!}{\pi(p+|l|)!}}\frac{1}{w(z)}\left(\frac{\sqrt{2}\rho}{w(z)}\right)^{|l|}L_p^{|l|}\left(\frac{2\rho^2}{w(z)^2}\right)\exp\left[-\frac{\rho^2}{w(z)^2}\right],\\&\times\exp\left\{-ik_{p,l,s}z\left[1+\frac{\rho^2}{2(z^2+z_R^2)}\right]\right\}\exp\left[i(2p+|l|+1)\theta_G(z)\right]\end{aligned}\tag{3}$$

where $w(z)=w_0\sqrt{1+(z/z_R)^2}$, w_0 is the beam waist, $z_R=\pi w_0^2/\lambda$ is the Rayleigh range, $\theta_G(z)=\tan^{-1}(z/z_R)$ is the Gouy phase, $k_{p,l,s}$ is the wave number, and $L_p^l(\cdot)$ represents the associated Laguerre polynomials. The wave number can be written in terms of the effective length L as $k_{p,l,s}L=\pi\left[s+(2p+|l|)(\Delta f_T/\Delta f_L)\right]$, where $\Delta f_L=c/2L$ is the longitudinal mode spacing and Δf_T is the transverse mode spacing. For an empty resonator consisting of one spherical mirror with radius of curvature R and one plane mirror, the bare ratio between the transverse and the longitudinal mode spacing is given by $\Delta f_T/\Delta f_L=(1/\pi)\cos^{-1}\left(\sqrt{1-L/R}\right)$. Experimental observations show that when the $\Delta f_T/\Delta f_L$ ratio is close to a simple fraction, the longitudinal-transverse coupling leads to frequency locking among different transverse modes, aided by different longitudinal orders to be the degenerate states [18]. In this work, $\Delta f_T/\Delta f_L=1/3$ was achieved, demonstrating that the nonplanar geometric modes were localized on six individual beams. The coherent optical wave propagating in clockwise and counterclockwise directions is expressed as $E_R(\rho,\phi,z)+E_L(\rho,\phi,z)$ by considering the standing wave in the cavity. Here,

$$E_R(\rho,\phi,z)=\sum_{k=-M}^{M}C_k^M e^{il\phi}\Phi_{p_0,l_0+3k,s_0-k}(\rho,z),\tag{4}$$

$$E_L(\rho,\phi,z)=\sum_{k=-M}^{M}C_k^M e^{-il\phi}\Phi_{p_0,l_0+3k,s_0-k}(\rho,z),\tag{5}$$

and $C_k^M=2^{-M}\begin{pmatrix}2M\\M+k\end{pmatrix}^{1/2}$ is the weighting coefficient. The parameter s_0 is an arbitrary number because the transverse pattern is independent of the factor. Figures 4(a)–4(f) present the numerical results for the transverse beam profiles described in Eqs. (4) and (5), with

#243787 Received 25 Jun 2015; revised 27 Jul 2015; accepted 29 Jul 2015; published 31 Jul 2015

$(p_0, l_0) = (0, 60)$ and $M = 4$ from $z = 0$ to the far field. The superposition of degenerate LG modes results in a nonplanar geometric mode. The condition $\Delta f_T / \Delta f_L = 1/3$ causes the

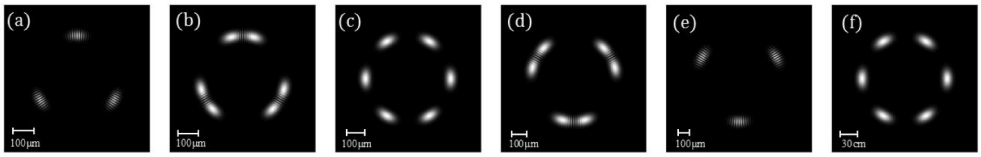

Fig. 4. Numerical results of superposed LG modes according to Eqs. (4) and (5) with $(p_0, l_0) = (0, 60)$ and $M = 4$ from $z = 0$ to the far field corresponding to experimental results in Fig. 1. The scale bars represent $100\,\mu m$ in (a)-(e) and $30\,cm$ in (f).

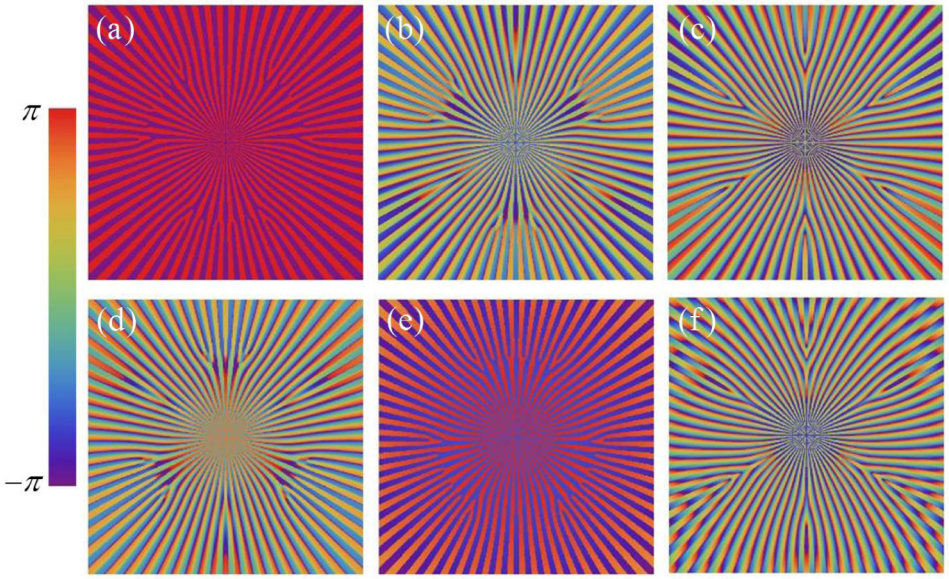

Fig. 5. Phase distribution of the superposed LG modes corresponding to Fig. 4.

localization of transverse optical waves at six spots in the azimuthal direction. The numerical results agree well with the experimental results presented in Figs. 1(a)–1(f). Figures 5(a)–5(f) show the evolution of the corresponding phase distribution of the superposed LG modes shown in Fig. 4. There are phase singularities embedded in the superposed LG modes during propagation. The LG mode associated with the spatial structure of the optical field has orbital angular momentum. The superposed LG modes of large azimuthal indices having large orbital angular momentum have potentially for wide applications.

5. Conclusion

We demonstrated the generation of orthogonally circular polarized states embedded in a nonplanar geometric mode by using a *c*-cut Nd:YVO_4 crystal. The conditions for generating orthogonally circular polarized states were quantized to match polarization continuity in the cavity. Numerical analyses of the polarization and tomogram are consistent with the experimental results. The results showed an interesting polarization distribution with three-dimensional orientation and provided useful insights for potential applications.

#243787 Received 25 Jun 2015; revised 27 Jul 2015; accepted 29 Jul 2015; published 31 Jul 2015

Acknowledgments

The authors thank the Ministry of Science and Technology for their financial support of this research under Contract No. MOST 101-2112-M-003-001-MY3.

#243787 Received 25 Jun 2015; revised 27 Jul 2015; accepted 29 Jul 2015; published 31 Jul 2015